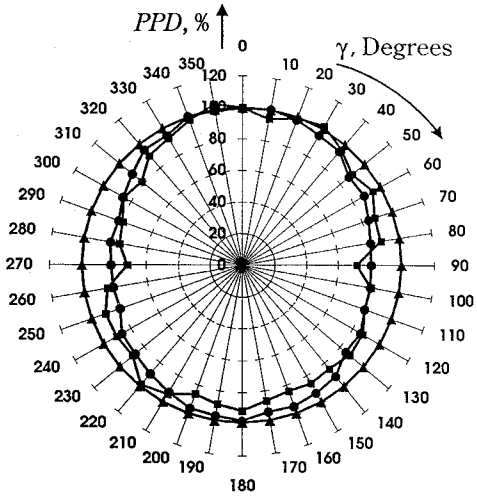

Fig. 3 Comparison between present PPD simulations and experimental measurements and Eq. (1), $V_f/V_p = 2.1$, $I = 18.1\%$; —■—, experimental; —●—, computational; and —▲—, Eq. (1).

the potential error magnitudes associated with angle bias. The effect of turbulence is also shown in comparing Figs. 2a and 2b. As would be expected, the increased turbulence tends to increase the PPD when the mean flow angle is close to parallel to the fringe planes. However, the PPD is slightly reduced when the mean flow angle is close to perpendicular to the fringe planes.

Of particular interest are the results shown in Fig. 3, which were obtained using $V_f/V_p \cong 2$. As a rule of thumb, LV users typically use this ratio to ensure uniform instrument response for all flow angles, based on predictions of the Whiffen et al. theory. The data presented in Fig. 3 show that uniform instrument response is not achieved at $V_f/V_p = 2$. For optical and flow parameters that are representative of those present in this experimental setup, the simulation shows that, for practical limits of V_f/V_p, perfectly uniform response will not be achieved. For example, using these parameter values and $V_f/V_p = 4$, the simulation predicts a minimum PPD of 87% at a mean flow angle of 90 deg. Although this PPD is relatively high, it still does not ensure isotropic instrument response.

Conclusions

A combined experimental/computational study investigating angle bias errors in laser velocimetry measurements has been performed. Experimental and computational results matched well, and indicate that the previously published theory overestimates the probability of particle detection (PPD), thus underestimating the potential error magnitudes associated with angle bias. The PPD overestimation in the theory arises primarily because the theory was developed using a two-dimensional, geometric probe volume cross section. The probability of particle detection is dependent on a large number of parameters and is too complex to quantitatively model in two geometrical dimensions. Even so, the theory remains useful in its simplicity in qualitatively predicting PPD profiles.

The results have also shown that the probability of particle detection is nonisotropic for fringe velocity/particle velocity ratios of approximately 2. Most LV researchers use this criteria to ensure uniform polar response of the instrument. Simulations have shown that, for practical configurations of the experimental setups used in this study, perfectly isotropic response will not be achieved. Rather, the instrument response will remain slightly dependent on the mean flow angle.

For single-component LV systems, or systems not acquiring three-component coincident measurements, angle bias cannot be corrected for. For three-component systems acquiring coincident measurements, it is not likely that a postprocessing correction scheme can be applied to compensate for angle bias. More importantly, the user should recognize what flow angles can be measured isotropically under the conditions present and realize the accuracy of the results obtained are limited by this instrument characteristic.

Acknowledgments

This work was performed under the auspices of Grant NGT-50868 provided through the NASA Langley Research Center while the first author was in residence at West Virginia University. The authors wish to thank James F. Meyers for suggesting the research presented in this paper.

References

[1]Edwards, R. V., Adrian, R., Boutier, A., Dybbs, A., Eaton, J., George, W., Meyers, J., Stevenson, W., and Yanta, W., "Report of the Special Panel on Statistical Particle Bias Problems in Laser Anemometry," *Journal of Fluids Engineering*, Vol. 109, June 1987, pp. 89–93.

[2]Whiffen, M. C., Lau, J. C., and Smith, D. M., "Design of LV Experiments for Turbulence Measurements," *Laser Velocimetry and Particle Sizing, Proceedings of the Third International Workshop on Laser Velocimetry*, edited by H. D. Thompson, and W. H. Stevenson, Hemisphere, Washington, DC, 1979, pp. 197–207.

[3]Meyers, J. F., and Walsh, M. J., "Computer Simulation of a Fringe Type Laser Velocimeter," *Proceedings of the Second International Workshop on Laser Velocimetry*, Purdue Univ., West Lafayette, IN, 1974, pp. 471–506.

[4]Anon., *Laser Doppler Velocimetry Components Catalog*, TSI, Inc., St. Paul, MN, 1988, p. 20.

[5]Fleming, G. A., "Error Analyses of Laser Velocimetry Measurements," MSME Thesis, Dept. of Mechanical and Aerospace Engineering, West Virginia Univ., Morgantown, WV, May 1993.

[6]Fleming, G. A., and Kuhlman, J. M., "Investigations of LV Statistical Data Bias Resulting From Flow Angularity and Counter Processor Thresholding," AIAA Paper 94-0040, Jan. 1994.

Shape Control of Plates Using Piezoceramic Elements

K. Ghosh*
Rochester Hills, Michigan 48307
and
R. C. Batra†
Virginia Polytechnic Institute and State University, Blacksburg, Virginia 24061-0219

Introduction

THE use of piezoceramic elements to control the vibrations of a beam has been extensively studied; see, for example, Baz and Poh.[1] However, their use to control the shape and vibrations of a thin plate has received less attention. We show here that the deflections of the centerline of a simply supported plate and the tip deflection of a cantilever plate, both deformed quasistatically, can be controlled by applying suitable voltages to the PZTs. The voltage to be applied to the actuators as a function of the surface area covered by them in the former case and as a function of their distance from the free end for the latter case is depicted graphically.

Formulation of the Problem

We consider a fiber-reinforced laminated composite plate with piezoelectric ceramic (PZT) elements bonded symmetrically to its top and bottom surfaces (Fig. 1), assume that the plate is symmetric about the midplane, and use the first-order shear deformation theory to study its infinitesimal elastic deformations. The adhesive between the PZT and the plate is assumed to be of negligible thickness, and displacements and surface tractions across the interfaces between the PZTs and the plate are taken to be continuous. The constitutive

Received July 29, 1994; revision received Feb. 6, 1995; accepted for publication Feb. 20, 1995.

*Engineer, 368 Woodside Ct., Bldg. 3, Apt. 31.

†Clifton Garvin Professor, Department of Engineering Science and Mechanics.

equations for both the material of the plate and the piezoceramic can be written as

$$\{\sigma\} = [C]\{\epsilon\} - [e]^T\{E\} \tag{1}$$

$$\{D\} = [e]\{\epsilon\} + [\xi]\{E\} \tag{2}$$

where σ is the stress tensor, ϵ the infinitesimal strain tensor, C the material elasticity matrix, e piezoelectric constants, D the induction vector, ξ dielectric permittivity, and E the electric field vector. As is commonly done in thin plate theory, we set $\sigma_{33} = 0$ and $\epsilon_{33} = 0$ (see Fig. 1 for the choice of coordinate axes). Depending upon the material symmetries, many elements of the 5×5 matrix C, 5×3 matrix e, and the 3×3 matrix ξ equal zeros; see Halpin.[2] We note that the induction vector D is related to the electric field vector E through Eq. (2) and $E = -\text{grad}V$ where V is the applied voltage. We assume that the displacement u of any point of the plate can be expressed in terms of the displacement u^0 of the corresponding point in its midplane by

$$u_i(x_1, x_2, x_3, t) = u_i^0(x_1, x_2, t) + (1 - \delta_{i3})x_3\phi_i(x_1, x_2, t)$$

$$i = 1, 2, 3 \tag{3}$$

where δ_{ij} is the Kronecker delta; ϕ_1 and ϕ_2 equal, respectively, the angles of rotation of the normal to the midsurface of the plate about the x_2 and x_1 axes, and ϕ_3 is taken to vanish identically. Using the strain-displacement relations, and integrating Eq. (1) and the product of both its sides with x_3 over the thickness of the plate, we obtain relations among the forces and moments acting at a point and the midsurface strains ϵ^0 and rotations ϕ.

Instead of working with the deflection equation for a plate, we start with the balance of linear momentum and the Maxwell equation, derive their weak forms, which incorporate the natural boundary conditions, and arrive at (see Ghosh[3])

$$\boldsymbol{KU} = \boldsymbol{F} + \boldsymbol{F}_c \tag{4}$$

where $\boldsymbol{U}$ is the matrix of extended displacements defined at points on the midsurface of the plate, $\boldsymbol{K}$ the stiffness matrix, $\boldsymbol{F}$ the resultant force corresponding to the applied loads, and $\boldsymbol{F}_c$ the force exerted by the PZTs onto the plate. Here we consider the case of a uniform voltage applied to the thin PZTs; therefore, the Maxwell equation is identically satisfied almost everywhere.

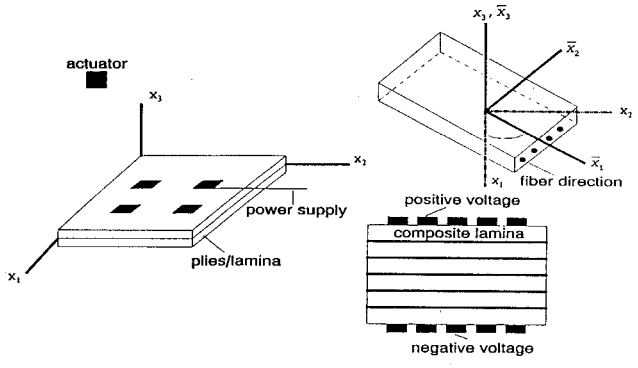

Fig. 1 Schematic sketch of the plate with PZTs.

Results and Discussion

We have developed a finite element code employing four-noded Lagrangian elements that can analyze the preceding problem. All nonzero elements of the stiffness matrix except those corresponding to shearing are evaluated by using the 2×2 Gaussian quadrature rule, and those corresponding to shearing are evaluated by using the one-point quadrature rule and are multiplied by the shear correction factor of 5/6. When computing numerical results, we assigned the following values to various material parameters. When the plate is made of aluminum, it is taken to be homogeneous and isotropic with Young's modulus $E = 65$ GPa and Poisson's ratio $\nu = 0.3$. For a T300/976 graphite/epoxy plate, the material properties with respect to the local principal axes are taken to be $E_{11} = 150$ GPa, $E_{22} = E_{33} = 9$ GPa, $\nu_{12} = \nu_{13} = 0.3$, $G_{12} = G_{31} = 7.1$ GPa, and $G_{23} = 2.5$ GPa.

For the G1195 piezoceramic PZT, we take $E_{11} = E_{22} = E_{33} = 63$ GPa, $\nu_{12} = \nu_{23} = \nu_{13} = 0.3$, $G_{12} = G_{23} = G_{13} = 24.2$ GPa, $e_{31} = 16.6$ pm/V, and $\xi_{11} = \xi_{22} = \xi_{33} = 15.2$ nf/m.

The boundary conditions considered for different support conditions are as follows: clamped edge—$u_i^0(x_1, x_2) = \phi_i(x_1, x_2) = 0$, $(x_1, x_2) \in \Gamma_{0e}$; simply supported edge parallel to x_1 axis—$u_2^0(x_1, x_2) = u_3^0(x_1, x_2) = \phi_1(x_1, x_2) = 0$, $(x_1, x_2) \in \Gamma_{0e}$; simply supported edge parallel to x_2 axis—$u_1^0(x_1, x_2) = u_3^0(x_1, x_2) = \phi_2(x_1, x_2) = 0$, $(x_1, x_2) \in \Gamma_{0e}$; and free edge—none. Here Γ_{0e} is the part of the boundary of the midsurface on which essential boundary conditions are prescribed.

The developed code has been validated by 1) comparing the computed x_3 displacement of the centroid of a simply supported rectangular aluminum plate with the corresponding analytical value

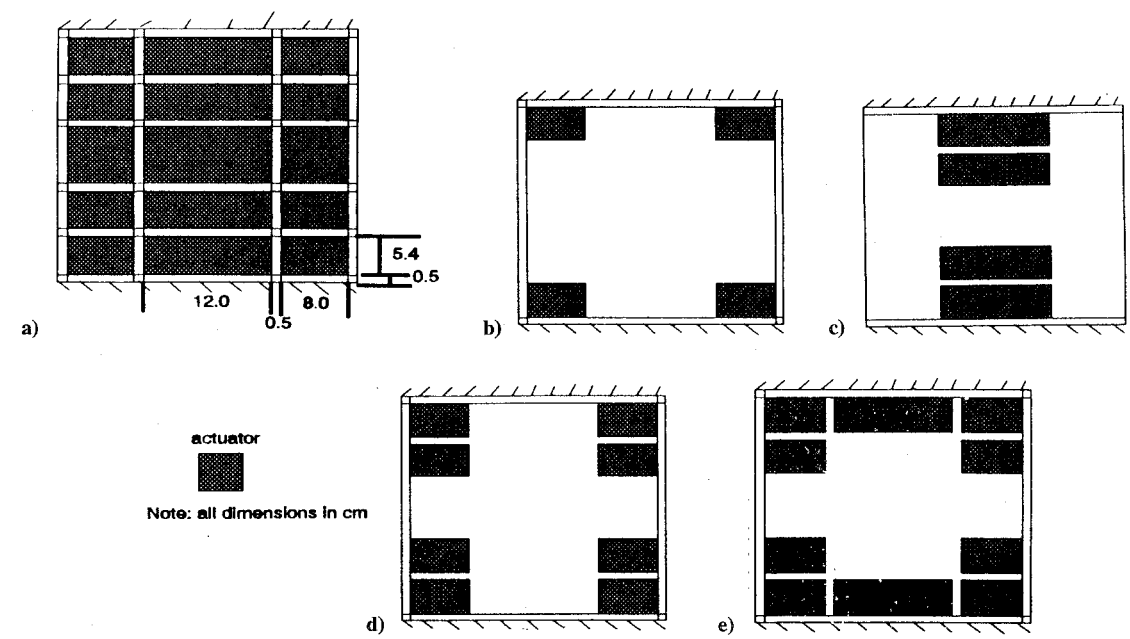

Fig. 2 Set up for the "smart" plate.

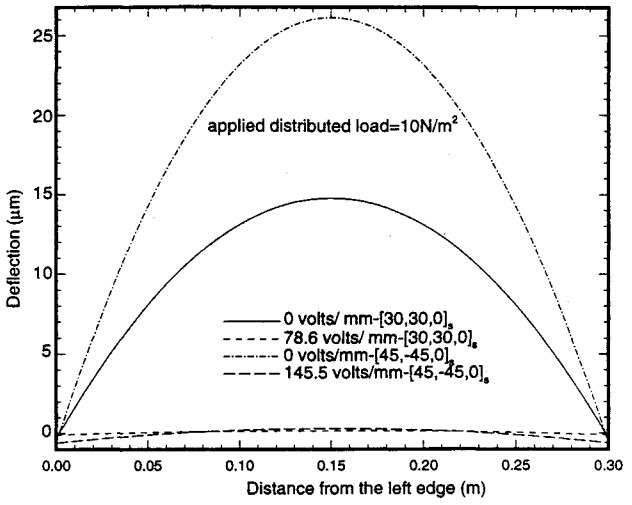

Fig. 3 Deformed shapes of the centerline of a simply supported plate for two different orientations of fibers both with and without actuators applying surface forces.

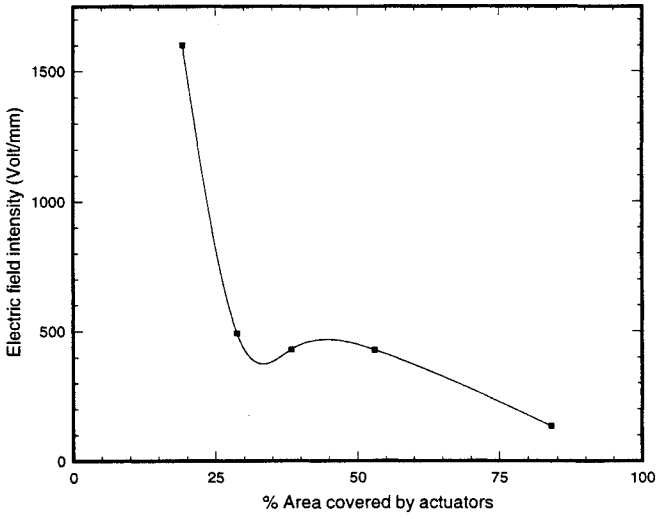

Fig. 4 Electric field intensity required to suppress the deflections of the centerline of a simply supported aluminum plate vs the surface area covered by the actuators.

and 2) comparing deflection of points on the centerline of a 0.292 × 0.152 m rectangular T300/976 graphite/epoxy 0.83-mm-thick composite cantilever plate with 0.25-mm-thick G1195 PZTs affixed symmetrically to its top and bottom surfaces with those reported by Crawley and de Luis.[4] In each case, the two sets of results were very close to each other.

We now investigate whether or not the deformed shape of a simply supported plate can be controlled by applying a voltage to the PZTs bonded symmetrically to its top and bottom surfaces. We consider a 0.3 × 0.3 m simply supported graphite/epoxy-1.8-mm-thick plate with PZT actuators placed on the top and bottom surfaces and subjected to 10 N/m² uniformly distributed load on the top surface; the setup is shown in Fig. 2. We note that the deformations of the plate are symmetrical about the two centroidal axes when no voltage is applied to the PZTs and also when equal and opposite voltages are applied to the PZTs that are located symmetrically about the centroidal axes. Figure 3 depicts the deformed shapes of the centerline of the plate for four different cases; the fiber orientations and the voltages applied are listed in the figure. It is clear that the forces and moments exerted by the PZTs are enough to suppress the deflection of the centerline of the plate. When a plate identical to the graphite/epoxy plate considered herein was made of aluminum, a voltage of 135 V/m applied to the PZTs eliminated the deflection of every point on its centerline.

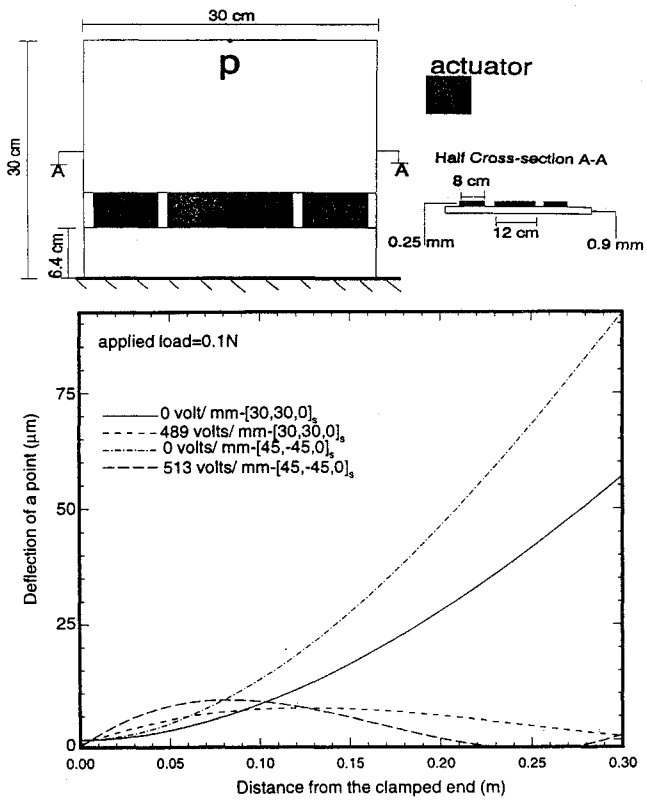

Fig. 5 Deformed shapes of the centerline of a "smart" cantilever plate both with and without actuators applying surface forces.

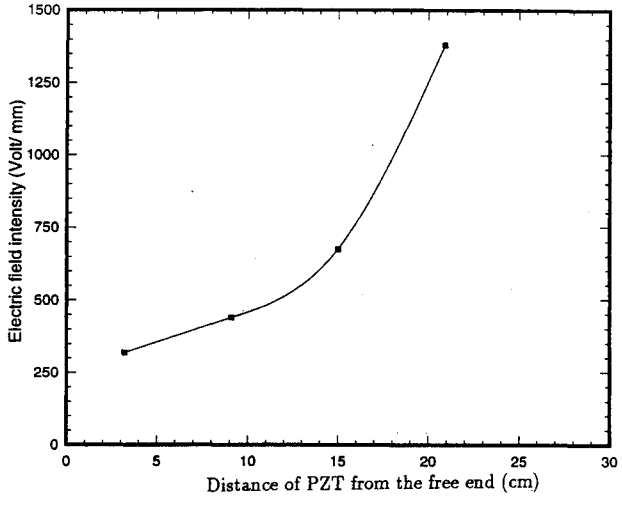

Fig. 6 Electric field intensity required to suppress the tip deflection of a cantilever plate vs the distance of PZTs from the free end.

Since PZTs are assumed to exert uniformly distributed forces on the surfaces where they are glued to the plate, the voltage to be applied to them will depend upon the plate surface area covered by the PZTs. With PZTs placed symmetrically about the two centroidal axes, their numbers and sizes were varied so as to cover 19.2–84% of the plate surface; Figs. 2a–2e depict the PZTs when the surface area covered by them equals 84, 19.8, 28.8, 38.4, and 53% respectively. For the square 0.3 × 0.3 m simply supported 1.8-mm-thick aluminum plate, Fig. 4 shows that the electric field intensity decreases noticeably with an increase in the surface area covered by the PZTs. For the fixed surface area covered by the PZTs, it was found that the electric field intensity to be applied to the PZTs to suppress the deflection of points on the centerline of the simply supported plate is an affine function of the intensity of the uniformly distributed load. The slope of the line depends upon the material of the plate and of

the PZTs, the surface area covered by the PZTs, plate dimensions, and the boundary conditions at the edges of the plate. This linear relationship between the intensity of the uniformly distributed load and the requisite voltage is to be expected since the deflection of a point is directly proportional to the load intensity and magnitude of surface forces is proportional to the voltage applied to the PZTs.

We now study the deformations of a cantilever plate with the objective of controlling the deflection of point P located at the center of the free end of the plate; see Fig. 5. It is clear from the results depicted in Fig. 5 that by applying proper voltage to the PZTs the deflection of point P can be made zero. For the cantilever aluminum plate, the voltage to be applied to the actuators to nullify the deflection of point P equaled 439.5 V/mm. We note that the deflection of other points near the fixed end is increased but that of those near the free end is decreased when the PZTs are activated. Keeping the sizes and relative locations of the three PZTs fixed, they were moved horizontally along the x_1 axis. The variation of the electric field intensity with the location on x_1 axis of the PZTs required to make the deflection of point P zero when a point load of 0.1 N is applied at P is shown in Fig. 6. It is apparent that the voltage to be applied to the PZTs increases sharply as the PZTs are moved towards the fixed end of the plate.

Acknowledgments

This work was supported by the U.S. Army Research Office Grant DAAH 04-93-G-0214 to the University of Missouri–Rolla and a matching grant from the Missouri Research and Training Center; the Virginia Polytechnic Institute and State University acted as a subcontractor.

References

[1]Baz, A., and Poh, S., "Performance of an Active Control System with Piezoelectric Actuators," *Journal of Sound and Vibration*, Vol. 126, No. 2, 1988, pp. 327–343.

[2]Halpin, J. C., *Primer on Composite Materials: Analysis*, Technomic, Westport, CT, 1984.

[3]Ghosh, K., "Shape Control of Plates Using Piezoceramic Elements," M.S. Thesis, Univ. of Missouri–Rolla, MO, Aug. 1994.

[4]Crawley, E. F., and de Luis, J., "Use of Piezoelectric Actuators as Elements of Intelligent Structures," *AIAA Journal*, Vol. 25, 1987, pp. 1373–1385.

Thermal Stresses in Eccentrically Stiffened Composite Plates

Z. C. Xi,* L. H. Yam,† and T. P. Leung‡
Hong Kong Polytechnic University, Hung Hom, Kowloon, Hong Kong

Introduction

FIBER reinforced composite materials have found wide applications in aerospace structures. Because these structures are often subjected to thermal loadings, their thermal stress analysis is quite important. The thermal stresses in bare composite plates have been well studied.[1] Recently, the thermally induced geometrically nonlinear response of symmetrically laminated composite plates was investigated by Meyers and Hyer.[2] The formulation of stiffness, thermal expansion, and thermal bending for stiffened composite panels was presented by Collier.[3]

The objective of this Note is to present a method for predicting thermally induced deformations and stresses in eccentrically stiffened composite laminates. The constitutive relations of a laminated composite stiffener are derived. Thermal effect and transverse shear deformation are included in the formulation. Numerical results are obtained for an eccentrically stiffened composite laminate subjected to a temperature change that is uniform within the plane of the plate but has a linear gradient through the thickness. The differences of thermal behaviors between stiffened and bare composite laminates are discussed.

Formulation

By using the first-order shear deformation theory, the laminate constitutive relations can be written in the form

$$\begin{Bmatrix} N \\ M \\ Q \end{Bmatrix} = \begin{bmatrix} A & B & 0 \\ B & D & 0 \\ 0 & 0 & A_s \end{bmatrix} \begin{Bmatrix} \varepsilon \\ \kappa \\ \gamma \end{Bmatrix} - \begin{Bmatrix} N^T \\ M^T \\ 0 \end{Bmatrix} \tag{1}$$

where $\{N\}^t=[N_x\ N_y\ N_{xy}]$, $\{M\}^t=[M_x\ M_y\ M_{xy}]$, and $\{Q\}^t=[Q_y\ Q_x]$ are vectors of the in-plane forces, moments, and transverse shear forces, respectively. Here, $\{N^T\}$ and $\{M^T\}$ are vectors of thermal forces and moments, respectively. The relations between the laminate stiffnesses $[A]$, $[B]$, $[D]$, $[A_s]$ and the ply engineering properties are given in Ref. 4.

When transverse shear deformation is considered, the constitutive relations of a thin, flat, bladelike laminated composite stiffener can be expressed as follows:

$$\begin{Bmatrix} N^s \\ M_x^s \\ M_{xy}^s \\ Q^s \end{Bmatrix} = \begin{bmatrix} A^s & B_1^s & B_6^s & 0 \\ B_1^s & D_{11}^s & D_{16}^s & 0 \\ B_6^s & D_{16}^s & D_{66}^s & 0 \\ 0 & 0 & 0 & A_s^s \end{bmatrix} \begin{Bmatrix} \varepsilon^s \\ \kappa_x^s \\ \kappa_{xy}^s \\ \gamma^s \end{Bmatrix} - \begin{Bmatrix} N^{sT} \\ M_x^{sT} \\ M_{xy}^{sT} \\ 0 \end{Bmatrix} \tag{2}$$

where N^s, M_x^s, M_{xy}^s, and Q^s are the axial force, bending moment, twisting moment, and transverse shear force, respectively. The stiffener stiffnesses are defined as

$$\left(A^s, A_s^s\right) = \int_{-h^s/2}^{h^s/2} \left(Q_{11}^s, 5/6Q_{55}^s\right) b\, \mathrm{d}z$$

$$\left(B_1^s, B_6^s\right) = \int_{-h^s/2}^{h^s/2} \left(Q_{11}^s, Q_{16}^s\right) bz\, \mathrm{d}z \tag{3a}$$

$$\left(D_{11}^s, D_{16}^s, D_{66}^s\right) = \int_{-h^s/2}^{h^s/2} \left(Q_{11}^s, Q_{16}^s, Q_{66}^s\right) bz^2\, \mathrm{d}z \tag{3b}$$

where h^s and b are the depth and width of the stiffener, respectively. The thermal axial force and bending and twisting moments are given by

$$N^T = \int_{-h^s/2}^{h^s/2} \begin{bmatrix} Q_{11}^s & Q_{16}^s \end{bmatrix} \begin{Bmatrix} \alpha_x \\ \alpha_{xy} \end{Bmatrix} \Delta T\, b\, \mathrm{d}z$$

$$\begin{Bmatrix} M_x^T \\ M_{xy}^T \end{Bmatrix} = \int_{-h^s/2}^{h^s/2} \begin{vmatrix} Q_{11}^s & Q_{16}^s \\ Q_{16}^s & Q_{66}^s \end{vmatrix} \begin{Bmatrix} \alpha_x \\ \alpha_{xy} \end{Bmatrix} \Delta T\, bz\, \mathrm{d}z \tag{4}$$

where

$$Q_{11}^s = \bar{Q}_{11} - \bar{Q}_{12}^2/\bar{Q}_{22}, \qquad Q_{16}^s = \bar{Q}_{16} - \bar{Q}_{12}\bar{Q}_{26}/\bar{Q}_{22}$$

$$Q_{66}^s = \bar{Q}_{66} - \bar{Q}_{26}^2/\bar{Q}_{22}, \qquad Q_{55}^s = \bar{Q}_{55} - \bar{Q}_{45}^2/\bar{Q}_{44} \tag{5}$$

Here, ΔT is the temperature change from the reference temperature. The expressions for the ply stiffnesses $\bar{Q}_{ij}$ $(i, j = 1, 2, 4, 5, 6)$ and coefficients of thermal expansion α_x, α_{xy} in terms of the ply engineering properties are given in Ref. 4.

Received Feb. 5, 1994; revision received Aug. 10, 1994; accepted for publication Sept. 2, 1994.

*Ph.D. candidate, Department of Mechanical and Marine Engineering.
†Assistant Professor, Department of Mechanical and Marine Engineering.
‡Vice President.